Lateral reorganization of plasma membrane is involved in the yeast resistance to severe dehydration

Sebastien Dupont [a], Laurent Beney [a,*], Jean-Francois Ritt [b], Jeannine Lherminier [c], Patrick Gervais [a]

[a] Laboratoire de Génie des Procédés Microbiologiques et Alimentaires, AgroSup Dijon, Université de Bourgogne, 1, esplanade Erasme, 21000 Dijon, France
[b] Centre de Recherche en Infectiologie, Division Microbiologie, Université de Laval, Boulevard Laurier, Québec, Canada G1V 4G2
[c] UMR Plante-Microbe-Environnement Université de Bourgogne/1088 INRA/5184 CNRS, INRA, BP 86510, 21065 DIJON Cedex, France

ARTICLE INFO

ABSTRACT

In this study, we investigated the kinetic and the magnitude of dehydrations on yeast plasma membrane (PM) modifications because this parameter is crucial to cell survival. Functional (permeability) and structural (morphology, ultrastructure, and distribution of the protein Sur7-GFP contained in sterol-rich membrane microdomains) PM modifications were investigated by confocal and electron microscopy after progressive (non-lethal) and rapid (lethal) hyperosmotic perturbations. Rapid cell dehydration induced the formation of many PM invaginations followed by membrane internalization of low sterol content PM regions with time. Permeabilization of the plasma membrane occurred during the rehydration stage because of inadequacies in the membrane surface and led to cell death. Progressive dehydration conducted to the formation of some big PM pleats without membrane internalization. It also led to the modification of the distribution of the Sur7-GFP microdomains, suggesting that a lateral rearrangement of membrane components occurred. This event is a function of time and is involved in the particular deformations of the PM during a progressive perturbation. The maintenance of the repartition of the microdomains during rapid perturbations consolidates this assumption. These findings highlight that the perturbation kinetic influences the evolution of the PM organization and indicate the crucial role of PM lateral reorganization in cell survival to hydric perturbations.

© 2010 Elsevier B.V. All rights reserved.

1. Introduction

Liquid water is a requirement for life on Earth and is the main factor of interest for researchers looking for life on other planets. However, diverse organisms, including tardigrades, nematodes, yeasts, and higher and lower plants, can survive in a dehydrated environment for extended periods. The mechanisms by which cells survive extreme dehydration are important to biological research and for stabilizing cells for biotechnological applications. The long-term preservation of biological materials is currently based on severe dehydration of the cell environment (e.g., freezing, drying, and freeze-drying) [1–3]. Dehydration is nevertheless an abiotic stress that perturbs cells and threatens survival.

The effects on cells induced by hydric perturbations are mainly a function of the severity of the treatment, and the magnitude of the perturbation determines the quantity of water that flows out of the cells. In the low-amplitude range of dehydration, most micro-organisms adapt through active metabolic pathways. Osmoregulatory pathways encompass active processes such as the high-osmolarity glycerol-signaling system through which cells monitor and adjust the internal osmotic pressure and control their shape, turgor, and relative water content [4], which allow cells to grow in concentrated media. The maximal osmotic pressure for osmoregulation varies according to microbial species and is about 15 MPa for the yeast Saccharomyces cerevisiae (S. cerevisiae) [5]. Long-term preservation strategies exceed this limit and typically involve osmotic pressures between 150 and 300 MPa corresponding to water activity (a_w) of 0.34 and 0.15, respectively. In this range of extreme dehydration, active cell responses have never been detected and cell survival is challenged considerably by the physicochemical constraints induced by the low hydric status. The structures of macromolecules and macromolecular assemblies are altered in these conditions [6], and the decrease in the cytoplasmic space caused by water outflow increases the confinement of intracellular structures and promotes aggregation phenomena [7].

Among the vital structures affected by extreme dehydration, the plasma membrane is a major target because the phospholipid bilayer structure results largely from the interaction of the lipids with the cytoplasmic and extracellular fluids. Dehydration and consequential osmotic phenomena cause movement of large quantities of water across the membrane, decreasing cell volume. For example, during hyperosmotic shock, the volume of yeast S. cerevisiae can be reduced

by 60% within a few milliseconds [8]. This event increases the cell surface-to-volume ratio (s/v), causing plasma membrane deformations such as ruffles, wrinkles, and surface roughness [9,10]. The fluidity and structural arrangement of membrane lipids also change; for example, their mobility decreases and the transition from the liquid lamellar to gel or hexagonal phases can occur under conditions of low water content [11–13]. These phenomena are often mentioned to explain plasma membrane permeabilization and cell death during hydric stresses [14–16].

Biological membranes have long been considered to be a fluid mixture of lipids organized in a homogenous bilayer. However, many studies reported that the plasma membrane of eukaryotic cells is highly compartmentalized laterally and that the membrane displays lipid microdomains enriched in sterols, sphingolipids, and specific raft proteins [17,18]. Lipid microdomains, so-called lipid rafts, are proposed to function in several processes including endocytosis and protein trafficking. The plasma membrane of the yeast S. cerevisiae comprises two different nonoverlapping lateral plasma membrane compartments. The first is occupied by the protein Pma1 and is called MCP (membrane compartment occupied by Pma1p) [19] or RMC P (raft-based membrane compartment P) [20]. The second contains the arginine transporter Can1 and is named MCC (membrane compartment occupied by Can1p) or RMC C (raft-based membrane compartment C). Grossmann et al. [21] have shown that 21 proteins cluster within or associate with the MCC ergosterol-rich membrane compartment. In physiological conditions, when fused to GFP, these proteins form a patch at the cell surface. The effect of severe perturbations on the plasma membrane lateral organization has never been investigated.

Several studies have shown that decreasing the rate of perturbation improves cell survival after extreme dehydration. Such kinetic effect was observed during dehydrations performed by drying [22] or hyperosmotic treatments [13,23] and suggest that the structural evolution of the membrane depends on the dehydration rate. The effects of the kinetics concern essentially the rate of osmotic water transfer and potentially the physical reorganization of cellular structures during dehydration. In the present study, we endeavored to clarify the impact of the magnitude and the kinetic of dehydration on plasma membrane reorganization and cell survival. We used yeast cells because they experience hydric fluctuations in their natural environment and are a convenient model to investigate the effect of hyperosmotic perturbations in eukaryotic organisms. Three dehydration conditions were chosen: 30 MPa ($a_w = 0.8$), corresponding to a sublethal level but out of the osmoregulatory range, and 110 MPa ($a_w = 0.45$) and 166 MPa ($a_w = 0.3$), corresponding to severe dehydration close to the water status of dried cells. Dehydration was induced by progressively increasing the concentration of glycerol in the extracellular solution (slope) or within a few milliseconds (shock). This protocol allowed us to induce severe cell dehydration in a liquid medium, which is convenient for microscopic observations [24]. Functional and structural investigations of the plasma membrane are necessary to understand the mechanisms operating during dehydration perturbation. To this end, we used fluorescence microscopy (epifluorescence and confocal) to observe modifications of the yeast plasma membrane during dehydration [25]. These modifications included changes in plasma membrane permeability, Sur7-GFP (contained in MCC) repartition, and membrane delocalization. To better understand the effect of dehydration kinetic, we used transmission electron microscopy (TEM) in cases where the kinetics influenced the fluorescent staining and survival rates. Our results show that slow perturbations led to the lateral reorganization of the plasma membrane, which was associated with the preservation of plasma membrane integrity, whereas rapid perturbation did not allow this phenomenon. We conclude that time is required for membrane reorganization and that this event is crucial for cell survival in response to severe dehydration.

2. Materials and methods

2.1. Yeast strain and culture conditions

S. cerevisiae strain BY 4742 (Euroscarf, Frankfurt, Germany) was used in this study. Cells were grown aerobically at 25 °C in 250 mL conical flasks containing 100 mL of Malt Wickerham modified medium (MW) (Sigma-Aldrich, Saint Quentin Fallavier, France). The MW medium contained 10 g glucose, 3 g pancreatic peptone, 3 g yeast extract, and 1.5 g NaH$_2$PO$_4$ in 1 L of water–glycerol, which had an osmotic pressure of 1.4 MPa. This osmotic pressure has been recommended for the optimal growth of S. cerevisiae [26]. A subculture (1 mL) was transferred into a conical flask containing MW medium, and cultures were placed on a rotary shaker (New Brunswick Scientific, Edison, NY, USA) at 250 rpm for 24 h and allowed to grow to the early stationary phase. The final population was estimated at about 10^8 cells mL^{-1}.

Plasmid amplification was carried out in the Escherichia coli (E. coli) DH5α host, grown at 37 °C in Luria–Bertani medium supplemented with 100 µg/mL ampicillin. The S. cerevisiae transformants were selected on Yeast Nitrogen Base casa plates (0.67% Difco yeast nitrogen base without amino acids, 0.5% NH$_4$Cl, 1% glucose, 0.1% Difco Bacto Casamino acids, and 1.8% agar).

2.2. Yeast transformation

The strain BY4742 was transformed with the plasmid YIp211-SUR7GFP after linearization by Eco52I. This plasmid was a generous gift from W. Tanner (University of Regensburg, Cell Biology and Plant Physiology, Regensburg, Germany) and was first transferred into E. coli DH5α and selected on Luria–Bertani plates supplemented with ampicillin (100 µg/mL). The S. cerevisiae strain transformation with the linearized YIp211SUR7GFP plasmid was performed by the LiAc method [27].

2.3. Preparation of binary water–glycerol solutions of different osmotic pressures

The solute used in all experiments to perform hyperosmotic treatments was glycerol (Sigma-Aldrich).

The mass of solute to be added to 1000 g of distilled water to obtain the desired water activity (a_w) was calculated using the Norrish equation [28]:

$$a_w = (1 - X_s)e^{-KX_s^2},$$

where X_s is the molar fraction of the solute and K is the Norrish coefficient of the solute used to increase the osmotic pressure. For glycerol, $K = 1.16$ [29]. Osmotic pressure (π) is related to the water activity by the following equation:

$$\pi = \frac{-RT \ln a_w}{V_w},$$

where R is the universal gas constant (J mol^{-1} K^{-1}), T is the temperature (K) and V_w is the partial molar volume of water (m^3 mol^{-1}). Table 1 presents the quantity of glycerol used to prepare the solutions of different osmotic pressures.

Table 1
Preparation of binary water–glycerol solutions of different osmotic pressures.

Osmotic pressure (MPa)	Water activity	Glycerol weight (g) for 1000 g of water
1.4	0.99	51
15	0.9	513
30	0.8	1063
110	0.45	3986
166	0.3	6654

The osmotic pressure of all solutions was checked with a dew-point osmometer (Decagon Devices Inc., Pullman, WA, USA).

2.4. Osmotic treatments

Three levels of osmotic treatments were used: moderate (30 MPa), which is slightly higher than that allowing osmoregulation, and severes (110 and 166 MPa).

Samples (20 mL) of culture were centrifuged (5 min, 2200 $\times g$), washed twice in the binary water–glycerol mixture (1.4 MPa), and the pellets were resuspended in 10 mL of the same medium. For rapid perturbations (shock), 1 mL aliquots of this suspension were placed in microsample tubes, which were then centrifuged (10 min, 5100 $\times g$) and the supernatant was removed. Hyperosmotic shock was induced by quickly introducing 1 mL of a binary water–glycerol solution (final osmotic pressure of 30, 110, or 166 MPa) to the pellets. For the progressive perturbations (osmotic slope of 0.086 MPa s^{-1}), the external osmotic pressure was increased linearly by slowly adding pure glycerol to an agitated conical flask containing the initial cell suspension at 1.4 MPa; the glycerol solution was injected by a syringe pump (KD Scientific, Boston, MA, USA). The cells were maintained for various maintenance periods under hyperosmotic conditions before rehydration. For rapid rehydration, the hyperosmotic solution was removed from the microsample tube after centrifugation (10 min, 5100 $\times g$) and 1 mL of the binary water–glycerol solution (1.4 MPa) was introduced suddenly to the cell pellet. Progressive rehydration was performed using successive dilutions in solutions with decreasing osmotic pressure to 1.4 MPa.

Cell suspensions, rehydration solutions, and shock solutions were kept in an air-conditioned room at 25 °C. The temperature of the solutions was checked using a thermocouple.

2.5. Measurement of yeast viability

Yeast viability was estimated in triplicate by the CFU method. After osmotic treatment, fully rehydrated cells were diluted serially and the appropriate dilutions were plated in MW medium with 15 g L^{-1} of agar. CFU were counted after incubation for 36 h at 25 °C. The initial cell suspension was used as the control.

2.6. Fluorescence microscopy

Propidium iodide (PI) (Invitrogen, Carlsbad, CA, USA) was used to assess plasma membrane integrity. This probe stains nucleic acids after permeabilization of the plasma membrane. PI was dissolved in distilled water (10 mg mL^{-1}) to prepare the stock solution, and 200 μg of PI was used to stain 10^8 cells. PI was added to the cell suspension before, during, or 60 min after the dehydration shock and after rehydration (Fig. 8A). This protocol allowed us to estimate the changes in the membrane permeability during and after hydric perturbation. For staining during the hydric stress, the probe was added to the hyperosmotic solution before induction of the perturbation. A Nikon Eclipse TE 2000 E epifluorescence microscope (Nikon, Tokyo, Japan) with spectral camera Nuance CRI was used to observe cells. Images were acquired with a $\times 40$ (NA: 0.95) Plan Apo objective (Nikon) and collected with Nuance software (Nikon). Black and white images were captured to observe the total cell population. A monochromatic epifilter (540–580 nm and 600–660 nm excitation and emission wavelengths, respectively) was used to observe cells stained with PI.

N-(3-triethylammoniumpropyl)-4-(6-(4-(diethylamino)phenyl) hexatrienyl)pyridinium dibromide (FM 4-64) (Invitrogen) is a membrane probe that is not fluorescent in an aqueous medium and which has been extensively used to observe endovesiculation phenomena [30–32]. In our study, FM 4-64 was used to observe the delocalization of membrane lipids and changes in cell morphology. The dye was dissolved in distilled water (1 mg mL^{-1}) to prepare the

stock solution, and 10^8 cells were stained with 20 μg of FM 4-64. Before staining, yeast cells were placed in the 15 MPa water–glycerol solution to stop the natural endocytosis pathway, which could perturb the observations of membrane delocalization induced by hyperosmotic treatment. This low osmotic pressure had no impact on yeast viability. A Nikon Eclipse TE 2000 U microscope with multispectral confocal head D Eclipse C1 was used to observe the cells stained with FM 4-64. Excitation was performed at 488 nm with laser He/Ar and the emission signal was recovered between 550 and 700 nm. Images were acquired with a $\times 60$ (NA: 0.95) Plan Apo objective and a $\times 100$ (NA: 1.4) Plan Apo oil-immersion objective (Nikon), and collected with EZ-C1 software 3.50 (Nikon).

Sur7-GFP was visualized using the same confocal microscope. Images were acquired with a $\times 100$ (NA: 1.4) Plan Apo oil-immersion objective (Nikon), and collected with EZ-C1 software 3.50 (Nikon). Excitation was performed at 488 nm, and the emission signal was measured between 500 and 550 nm.

2.7. Electron microscopy

TEM was used to assess the yeast ultrastructure just after hyperosmotic slope and shock to 110 MPa. Concentrated yeast samples were fixed for 12 h at 4 °C with 3% glutaraldehyde and 2% paraformaldehyde in PBS for control cells (1.4 MPa) and in water–glycerol solution for cells subjected to 110 MPa osmotic pressure. Treated cells were fixed just after the end of the osmotic treatment. After washing, cells were postfixed with 0.5% OsO$_4$–0.1 M phosphate buffer, pH 7.2, for 1 h at 4 °C. Cells were dehydrated progressively in 30%, 50%, 70%, 90%, and 100% ethanol, 30 min for each step, impregnated with Epon, and polymerized at 60 °C for 48 h. Ultrathin sections (90 nm) were obtained using an Ultracut E ultramicrotome (Reichert, Depew, NY, USA) and contrasted with uranyl acetate and lead citrate. Polysaccharides were detected histochemically by the periodic acid–thiocarbohydrazide (TCH)–silver proteinate (PATAg) method described by Thiery [33]. Observations were performed on a Hitachi 7500 transmission electron microscope (operating at 80 kV) equipped with an AMT camera driven by AMT software (AMT, Danvers, MA, USA).

3. Results

3.1. Impact of hyperosmotic treatments on yeast viability
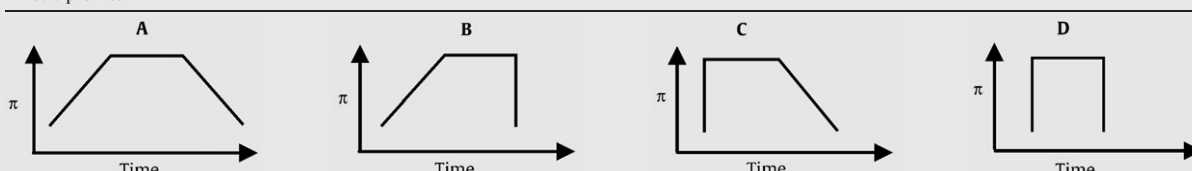
3.1.1. Kinetic and magnitude of hyperosmotic treatments influence the yeast survival

Cells were treated with the hyperosmotic conditions at 30, 110, or 166 MPa for 60 min and then rehydrated to 1.4 MPa. The dehydration and rehydration steps were achieved progressively or quickly according to 4 possible combinations (Table 2). For 30 MPa, the rates of dehydration and rehydration had almost no effect on yeast viability, which remained higher than 80%. For severe dehydrations, the survival rate depended on the kinetics of dehydration and rehydration. At 110 and 166 MPa, the best viabilities were observed after progressive dehydrations followed by progressive rehydrations (86.9% and 78.7%, respectively) and the weakest were observed when the two steps were performed quickly (12.5% and 0.3%, respectively). Intermediate viabilities were obtained after slope/shock and shock/slope cycles: 41.7% and 67.7%, respectively, for the treatments to 110 MPa, and 19.2% and 42.6%, respectively, for the treatments to 166 MPa. These results showed that the magnitude of the dehydration treatment influenced the cell viability. For severe perturbations (110 and 166 MPa), survival rates are strongly related to the perturbation kinetic of the dehydration and rehydration steps.

3.1.2. First minutes after a severe hydric shock are crucial for cell survival

The effect of maintenance periods in hyperosmotic conditions on cell viability was estimated by rapid rehydration at different times

Table 2
Impact of changes in the kinetics of dehydration and rehydration on yeast viability for treatments to 30, 110, and 166 MPa with a maintenance period of 60 min in hyperosmotic conditions.

Amplitude	Kinetic profiles			
	A	**B**	**C**	**D**
30 MPa	86.0% (3.6)	86.2% (3.9)	88.2% (8.4)	83.5% (2.5)
110 MPa	86.9% (11.6)	67.7% (4.7)	41.7% (12.7)	12.5% (9.1)
166 MPa	78.7% (3.6)	42.6% (3.6)	19.2% (1.1)	0.3% (0.2)

π corresponds to the osmotic pressure of the extracellular medium. (A) Slow dehydration and slow rehydration, (B) slow dehydration and rapid rehydration, (C) rapid dehydration and slow rehydration, and (D) rapid dehydration and rapid rehydration. Survival rate was measured using the CFU method after rehydration to 1.4 MPa. The SDs were calculated from three experiments.

after the hyperosmotic shock: 1, 15, and 60 min for 30 MPa, and 1, 2, 15, and 60 min for 166 MPa (Fig. 1). For 30 MPa shock, cell viability did not evolve significantly according to maintenance periods and remained close to 85%. This result indicates that the decrease of the survival rate occurs during the first minute after the shock and that the viability is not affected by the maintenance time. After osmotic shock at 166 MPa, cell viability decreased markedly with increasing maintenance time in hyperosmotic conditions. The viability was 48.9% when cells were rehydrated 1 min after the shock and declined to 38.7%, 3.6% and 0.3% for rehydration at 2, 15 and 60 min, respectively. These results suggest that events occurring during the first minutes after severe hyperosmotic shock influence the cell survival during the rehydration.

3.2. Plasma membrane internalization depends on the amplitude and the kinetic of hyperosmotic treatments

3.2.1. Arrest of endocytosis at 15 MPa

Endocytosis refers to the formation of vesicles in the cytosol from the plasma membrane. It is a rapid process that allows the internalization of extracellular fluids, particles, and plasma membrane proteins by invagination of the plasma membrane [32]. The yeast plasma membrane was stained by FM 4-64 and visualized using confocal microscopy to observe the membrane delocalization (Fig. 2). Initially, the probe was observed only in the plasma membrane. With

Fig. 1. Evolution of the viability of yeast cells during different maintenance periods after hyperosmotic shock to 30 MPa and 166 MPa. Viability was measured by the CFU method after rapid rehydration to 1.4 MPa. The cells were rehydrated for 1, 15, or 60 min after the shock to 30 MPa and for 1, 3, 15, or 60 min after the shock to 166 MPa. Error bars correspond to the SD calculated from three repeat experiments.

time and in iso-osmotic conditions corresponding to the osmotic pressure of the culture medium (1.4 MPa), the plasma membrane was internalized and reached intracellular compartments such as vacuoles after 60 min (Fig. 2C). The kinetic of the probe internalization is consistent with observations previously reported [34]. As endocytosis is an energy-dependent phenomenon [35], yeast placed in a 1.4 MPa water/glycerol solution possessed sufficient energetic resources. In our study, FM 4-64 staining was used to assess plasma membrane delocalization during hydric perturbations. It was necessary to arrest this phenomenon because it could disturb observations during progressive dehydration which required 30 min to reach 166 MPa. So we seek for non-lethal conditions which stopped this phenomenon. For that, we placed the cells at 15 MPa which corresponds to the limit level of yeast osmoregulation [5]. At this amplitude, staining by the FM 4-64 remained in the plasma membrane over time (Fig. 2D, E, and F).

3.2.2. Induction of plasma membrane internalization by severe hyperosmotic shock

Yeasts were observed at 1, 10, and 60 min after hyperosmotic treatments. The images obtained after hyperosmotic perturbations are presented in Figs. 3 and 4.

After shock or slope to 30 MPa, the staining by FM 4-64 appeared only in the plasma membrane, and the pattern was similar to that of cells before treatment (Figs. 3 and 4). Shocks to 110 and 166 MPa led to progressive plasma membrane internalization which occurred during the maintenance period in hyperosmotic conditions. Small spots of probe were visible close to the plasma membrane 10 min after the beginning of the treatment (Fig. 3F and I). The probe was internalized deeper in the cell with time and reached intracellular compartments such as vacuoles after 60 min (Fig. 3G and J). However, membrane internalization did not affect all the cells after the shock to 110 MPa contrary to the one to 166 MPa. Indeed, a minor part of cells (~20%) did not present intracellular FM 4-64 staining after 60 min time exposure (Fig. 3G). So, these results show that the shock to 30 MPa did not induce plasma membrane delocalization, whereas shocks to 110 and 166 MPa caused plasma membrane internalization. Progressive dehydrations to 110 and 166 MPa were characterized by a peripheral staining which did not evolve over time (Fig. 4). The plasma membrane was not internalized during the 60 min following the perturbations but presented a peculiar aspect. Spots of probe were observed in the plasma membrane at the end of the progressive dehydration; these spots may correspond to large wrinkles of membrane or vesicles that stayed close to the plasma membrane.

These original results showed that hyperosmotic shock to 110 and 166 MPa induced membrane internalization during the maintenance period in hyperosmotic conditions. For these high-osmotic pressure
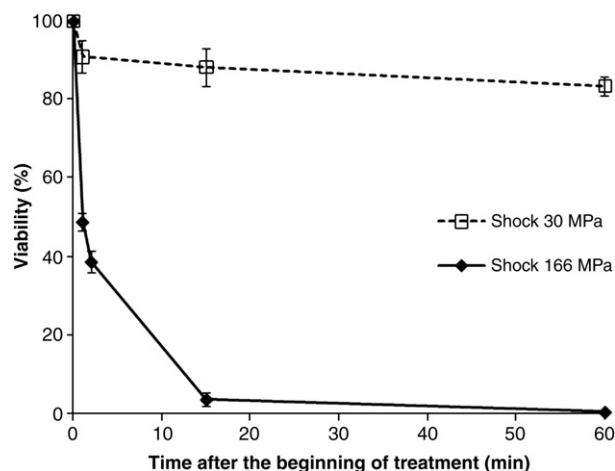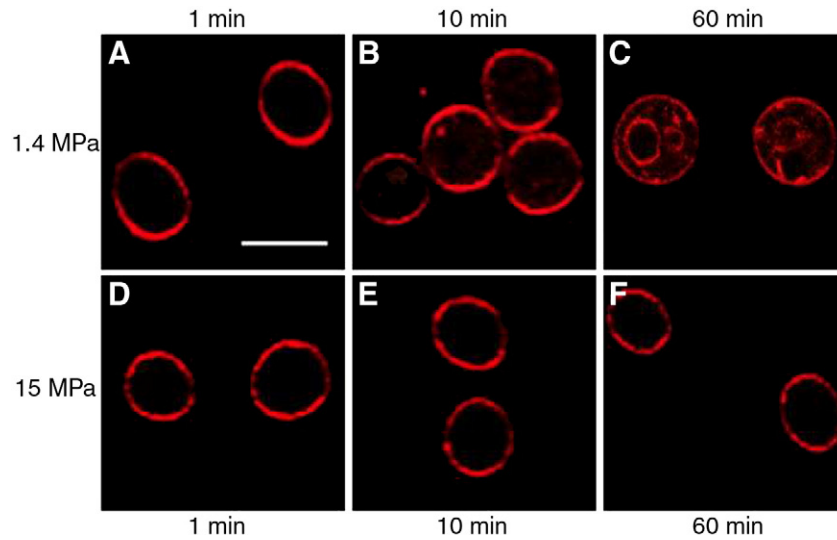
Fig. 2. Effect of an increase in osmotic pressure to 15 MPa on plasma membrane endocytosis. Representative confocal laser scanning microscopy images of yeast *Saccharomyces cerevisiae* showing evolution over the time of FM 4-64 staining in iso-osmotic conditions (A, B, and C) and after 15 MPa hyperosmotic treatment (D, E, and F) at 25 °C. Observations were performed 1, 10, and 60 min after the staining with the probe. Bar scale = 5 μm.

levels, the kinetic of dehydration influenced the morphological evolution of the plasma membrane.

3.3. Dehydration kinetic influences plasma membrane deformations

TEM was used to characterize ultrastructural changes in cases where the dehydration kinetic influenced the survival rate and the fluorescent staining by FM 4-64 (Table 2 and Figs. 3 and 4). As it was not possible to fix the cells at 166 MPa because of the high viscosity of the solutions, observations were performed on samples dehydrated to 110 MPa (Fig. 5). Cell fixation was performed just after the treatments

(slope or shock) to observe membrane modifications which occurred after the perturbations. Fixation of cells was performed with chemical fixation. This protocol can sometimes alter the structure of the plasma membrane with artificially tilted and profound invaginations, evoked by Stradalova et al. [36], caused by the osmotic effects of chemical fixatives [37]. These artifacts were not observed on the control cells and allowed reasonable comparative observations between the samples after slope and shock dehydrations.

Control cells presented an almost smooth plasma membrane with about ten curved membrane areas per cell median microscopic section that corresponded to invaginations of ~50 nm deep (Fig. 5A
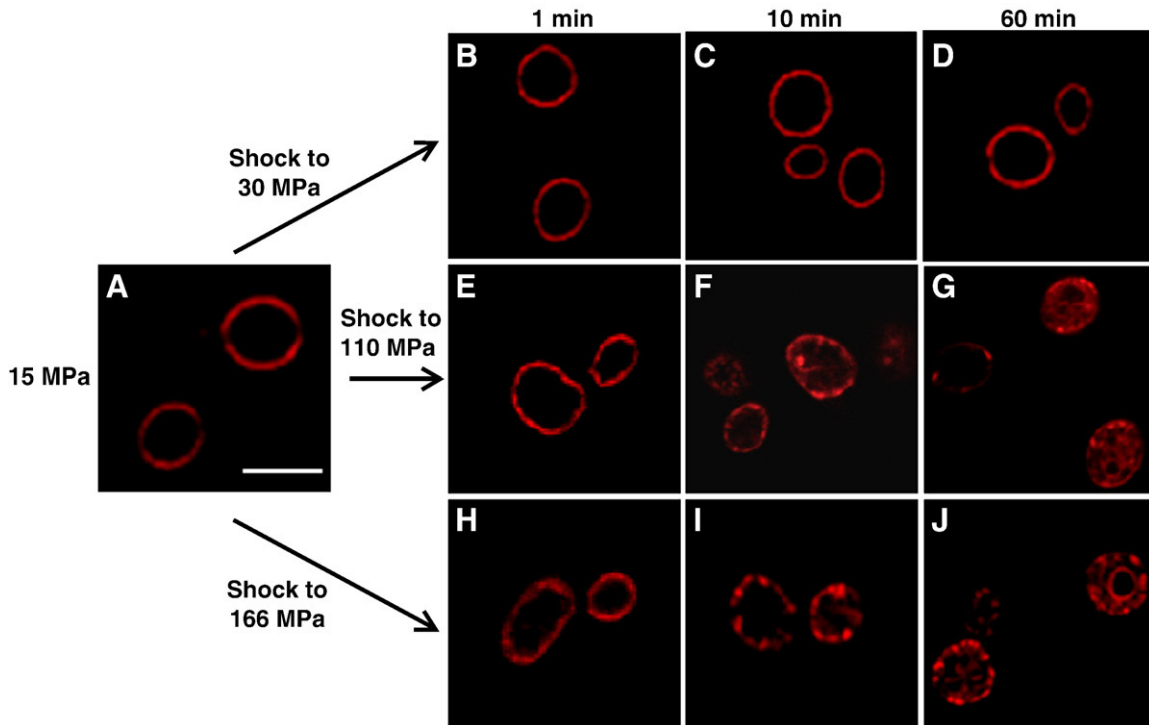

Fig. 3. Impact of hyperosmotic shocks on plasma membrane internalization. Representative confocal laser scanning microscopy images of yeasts *Saccharomyces cerevisiae* stained with the styryl dye FM 4-64 after hyperosmotic shocks to 30, 110, and 166 MPa carried out with glycerol. (A) Control cells in 15 MPa water/glycerol solution; (B), (C), and (D) correspond to cells after 30 MPa hyperosmotic shock; (E), (F), and (G) after hyperosmotic shock to 110 MPa and (H), (I), and (J) after hyperosmotic shock to 166 MPa. Cells were observed 1, 10, and 60 min after the shocks. Bar scale = 5 μm.
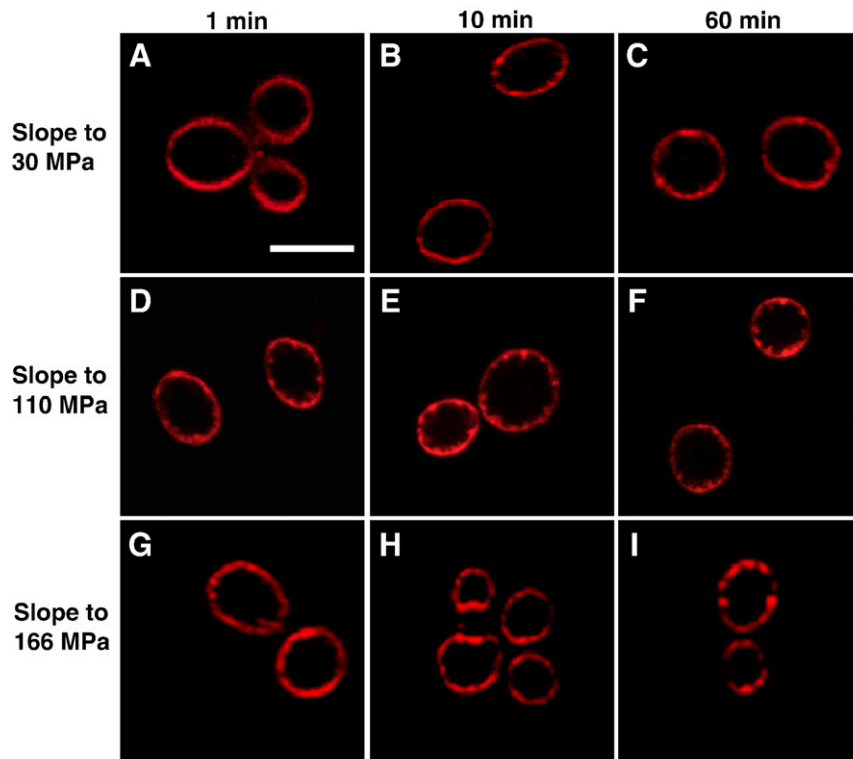
Fig. 4. Impact of hyperosmotic slopes on plasma membrane internalization. Representative confocal laser scanning microscopy images of yeasts *Saccharomyces cerevisiae* stained with FM 4-64 after hyperosmotic slopes of 30, 110, and 166 MPa carried out with glycerol. Progressive dehydrations were performed with a rate of 0.086 MPa s^{-1}. (A), (B) and (C) correspond to cells after slope to 30 MPa; (D), (E), and (F) after slope to 110 MPa and (G), (H), and (I) after slope to 166 MPa. Cells were observed 1, 10, and 60 min after the end of the slopes. Bar scale = 5 μm.

and B). Observations of superficial sections revealed that these invaginations presented a furrow-like aspect with a length of ~300 nm (data not shown). This type of invaginations has already been described and localized within MCC patches [36]. After the shock to 110 MPa, cells showed an undulated plasma membrane with deeper invaginations than in control cells. These invaginations were narrower at the base than at the tip and extended about 150 nm into the cytosol (Fig. 5D). After the slope condition to 110 MPa, membrane deformation was different: the invaginations were fewer but were longer (~400–500 nm) than in the case of the shock dehydration (Fig. 5E). They often appeared curl back toward, and in some cases even to fuse, with themselves or the cell surface (Fig. 5F).

In contrast to the observations after dehydration in vegetal cells [38], the cell wall remained in contact with the plasma membrane after the dehydration treatment, and the classical plasmolysis event was not observed. This can be explained by the many anchorage sites between the cell wall and plasma membrane in yeast and by the greater elasticity of the wall of yeast cells than in vegetal cells [39].

3.4. Progressive dehydration leads to lateral redistribution of Sur7-GFP

Effect of treatments to 166 MPa (progressive or rapid) on lateral distribution of Sur7-GFP was studied. In control cells, Sur7 proteins fused to GFP were not distributed homogeneously in the plasma membrane but were concentrated in discrete patches (Fig. 6A), as described previously [19,40]. Analysis of the fluorescence intensity profiles of the median optical sections gave an estimated mean number of patches at the median section of the control cells of 11 with a size of about 550 nm (Table 3). This number of patches is in agreement with previous observations [19]. MCC size of 300 nm which is smaller than the size estimated in the present study has been reported [20]. This difference could result from the blur introduced by micro-

scopic imaging and from the threshold used to estimate the domain size. After hyperosmotic shock to 166 MPa, the repartition of Sur7-GFP domains remained in distinct patches (Fig. 6B). The distance between the fluorescence intensity peaks on the membrane perimeter was smaller than that in control cells, indicating that the Sur7-GFP patches were positioned closer to each other. The size of the domains was also slightly decreased. Progressive dehydration to 166 MPa changed the distribution of the Sur7 proteins, and the plasma membrane did not exhibit small fluorescent patches, but larger fluorescent domains (Fig. 6C) with a mean size of about 1.1 μm (Table 3). The number of domains decreased from 11 in median cell sections of control cells and cells subjected to rapid dehydration (shock) to 6 distinct domains after progressive dehydration (slope). Progressive dehydration caused a redistribution of Sur7p from the patches, suggesting that lateral membrane reorganization occurred during this treatment. These results indicate that the dehydration kinetic influences the evolution of the repartition of Sur7p.

Effect of rehydration on Sur7p distribution was assessed by observation of cells after dehydration to 166 MPa followed by rehydration. Yeasts were treated according to a dehydration–rehydration cycle leading to low survival rate (shock–shock) or to a cycle conducting to high survival rate (slope–slope). After the shock–shock cycle, Sur7-GFP was localized in the cell cytosol and was not observed in the plasma membrane (Fig. 7A) and did not evolve with time (Fig. 7B). As Sur7p is a membrane protein, this aberrant localization could be explained by lysis of the cells during the shock rehydration. Just after the rehydration step of the slope–slope cycle, fluorescence of Sur7-GFP was observed in large and diffuse domains of the plasma membrane (Fig. 7C). Sur7-GFP regained the initial small patch distribution 90 min later (Fig. 7D) suggesting that MCC domain re-formation required time. These results show an influence of the rehydration kinetic on the structural evolution of the plasma membrane.
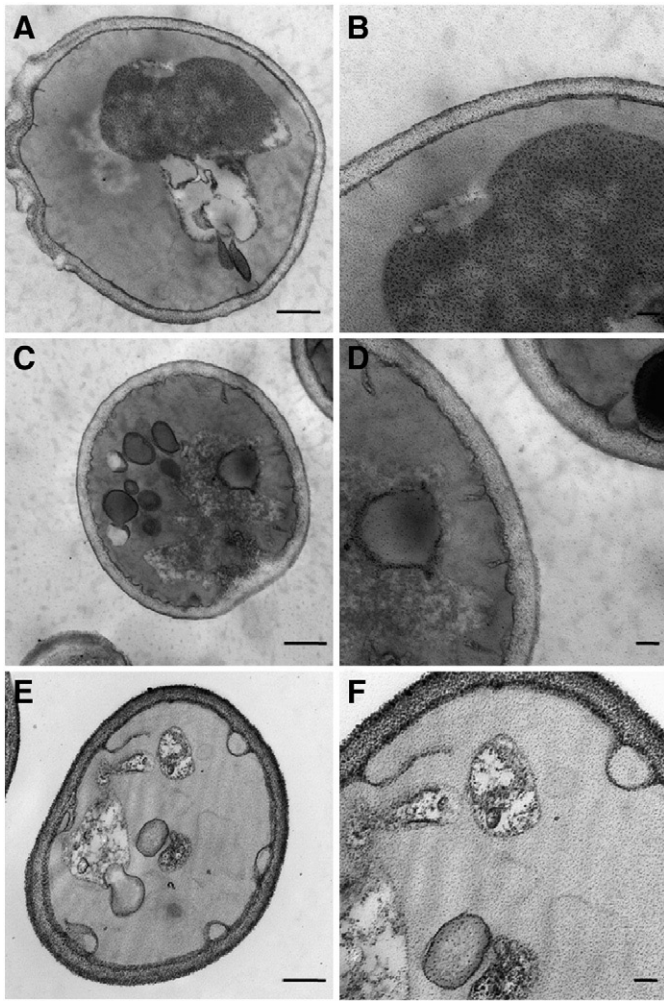
Fig. 5. Ultrastructure of yeast in the first moments after hyperosmotic treatments. TEM micrographs of representative yeast sections. Control cells (A and B), cells after shock to 110 MPa (C and D) and after slope to 110 MPa (E and F) were treated with Thiery reaction. Cells were fixed just after the hyperosmotic treatments. (A), (C), and (E): bar scale = 500 nm. (B), (D), and (F): bar scale = 100 nm.

3.5. Plasma membrane integrity is challenged both by dehydration and rehydration

The permeability of the plasma membrane of the yeast cell population was estimated with PI staining. The cells were labeled during, or 60 min after dehydration, and after rehydration in the high-osmotic pressure (166 MPa) condition in the slope and shock experiments (Fig. 8A). Dehydration led to permeabilization of some of the cells, and the proportion of cells affected was higher for shock (45.6%) than for slope (12.9%). The staining pattern was similar for staining performed during the perturbations and for staining performed 60 min after the maintenance period at 166 MPa. This result indicates that permeabilization occurred in the first minute of the treatments and persisted over the time. Shock rehydration, performed after 60 min maintenance, caused additional permeabilization of cells: proportion of permeabilized cells after rapid rehydration reached 86.4% and 55.2% for the dehydration achieved according to a shock or a slope, respectively (Fig. 8). These results suggest that the kinetics of dehydration and rehydration influence the membrane integrity of the plasma membrane. Thus, the two steps of the dehydration–rehydration cycle are critical for maintaining plasma membrane integrity.

4. Discussion

We have extended the findings of a previous study [16] on the impact of hyperosmotic stress on the plasma membrane by characterizing the structural and functional plasma membrane modifications following osmotic perturbations. We focused on the effects of the kinetic and the amplitude of hyperosmotic treatments on these alterations to understand the influence of these parameters on yeast survival. Several pieces of evidence are presented, which allow us to propose a scenario describing the events implied in survival and death of cells during hydric perturbations (Fig. 9).

4.1. Preservation of cell integrity and high survival rate after moderated dehydration (15 and 30 MPa)

Hyperosmotic treatment to 30 MPa led to a high survival rate of yeast (Table 2), and progressive and rapid dehydration to this level conducted to the same viability. This suggests that survival after mild dehydration is not dependent on the kinetics of dehydration and rehydration. Cell viability was not affected by the duration of the maintenance at 30 MPa before rehydration (Fig. 1). Thus, this osmotic level, slightly higher than the one allowing osmoregulation [5], corresponds to a condition where the cell growth is stopped but where the viability remains high. This suggests that the plasma membrane integrity is preserved over the time in this condition. Fluorescent staining by FM 4-64 showed a smooth and regular aspect of the yeast plasma membrane after the perturbation to 30 MPa (Figs. 3 and 4), similar to that in the control cells (Fig. 3A), which did not change with exposure time. Preservation of membrane integrity could be related to the maintenance of lipid order in the liquid phase. Indeed, the lipid phase transition from the liquid-crystalline to gel phase, which can destabilize the plasma membrane, has been reported to occur above 60 MPa in glycerol solutions for *S. cerevisiae* [12].

Experiments performed at 15 and 30 MPa showed that mild dehydrations, to levels higher than the ones allowing yeast osmoregulation [5], conducted to the arrest of plasma membrane endocytosis mechanism (Figs. 2 and 3). This active mechanism is time, temperature and energy dependent [35]. In our study, endocytosis was observed even if the yeasts were placed in water–glycerol at 1.4 MPa (Fig. 2). This suggests that an energetic insufficiency cannot be the cause of the observed arrest of endocytosis. Arrest of endocytosis is most probably related to the consequences of the decrease of hydric potential on macromolecular structure assemblies. For example, hyperosmotic treatments are known to cause depolymerization of the yeast cytoskeleton [41,42] which is required for plasma membrane endocytosis [43,44].

4.2. Severe hyperosmotic shocks (110 and 166 MPa) lead to cell death

Yeast viability was strongly affected by rapid and severe dehydrations (Table 2). Leaking of cellular content induced by plasma membrane permeabilization is often reported to explain cell death during hydric perturbation [11,14]. Membrane continuity is essential for maintaining many vital cellular functions that rely on membrane-bound proteins and electrochemical potentials, such as ATP synthesis. The results of the membrane permeability experiments (Fig. 8B) and those on viability (Table 2) confirm this hypothesis because the proportion of permeabilized cells was similar to that of dead cells. Staining by PI at different moments of dehydration–rehydration cycles allowed us to specify the critical phases for plasma membrane integrity (Fig. 8) and to draw the probable scenario explaining cell death during hydric treatments. This scenario is composed of two phases presented in Fig. 9A.

First, a part of cells are irreversibly permeabilized during the rapid volume variation phase caused by the osmotic shock (Fig. 8B).
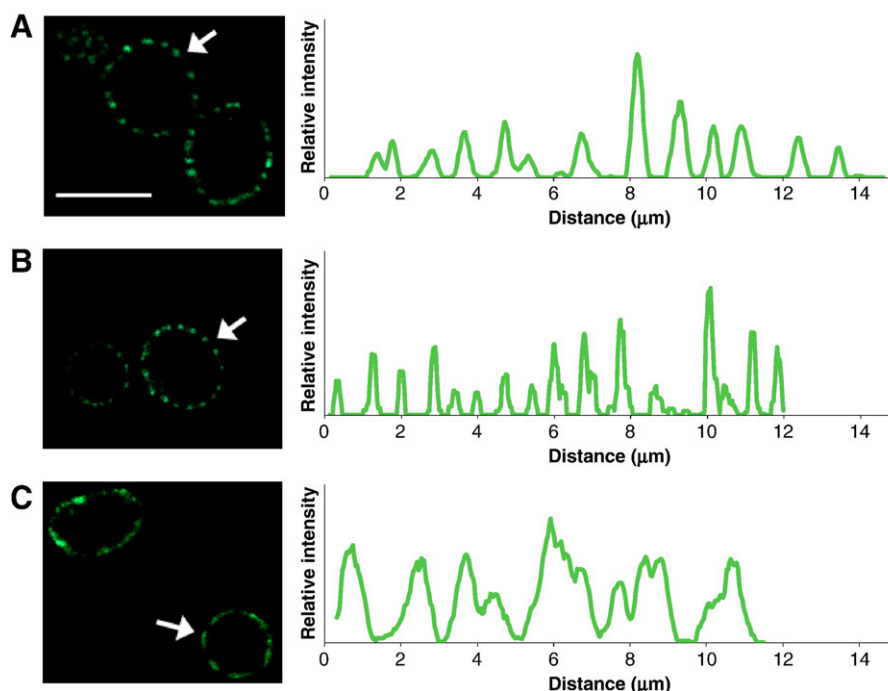
Fig. 6. Impact of dehydration kinetics to 166 MPa on Sur7-GFP domain repartition in the plasma membrane. (A) Control cells, (B) cells after rapid dehydration to 166 MPa, and (C) cells after progressive dehydration to 166 MPa. On the left of the figure, median optical sections through the cells are shown. On the right, representative fluorescence intensity profiles (diagrams) measured along the perimeter of the cells are shown. Each profile corresponds to the cell indicated by an arrow. A mean filter was applied on the plotted curves to reduce the noise present in the raw data, and the curves were normalized to the same maximum value. Bar scale = 5 μm.

Membrane permeabilization could be related to the phase transitions of lipids emerging around 60 MPa [12]. Such phenomenon is induced by the removal of water from polar head groups during dehydration [11] and affects the resistance of membranes to shear forces [45]. Moreover, rapid volume contraction may be critical because plasma membrane regions with too high curvature could experience the loss of the continuity of the lipid bilayer.

Rehydration step after maintenance period in hyperosmotic conditions is also critical for cell integrity. Maintenance period of 60 min followed by rapid rehydration conducted to an increase of the proportion of permeabilized cells (Fig. 8B). Higher survival rates were observed when the exposure times were brief (<15 min) (Fig. 1) suggesting that membrane integrity was preserved during rehydration for the short maintenance period in hyperosmotic conditions. Thus, permeabilization occurring during the rehydration phase is linked to events arising in the first minutes after the shock dehydration. During this period, progressive plasma membrane internalization was observed (Fig. 5). This phenomenon leads to reduction of the plasma membrane surface, which becomes insufficient during the rehydration step and leads to cell lysis when the cell volume increases (Fig. 9A). Plasma membrane rupture explains the abnormal intracellular location of Sur7-GFP observed after rapid rehydration (Fig. 7).

The relation between membrane internalization and cell death is supported by the higher survival rate after 110 MPa than 166 MPa which could be related to the absence or the insufficiency of membrane internalization for some cells at 110 MPa (Fig. 3G). Thus, plasma membrane internalization induced by hyperosmotic shock seems to be a key event in the induction of the cell death during the dehydration–rehydration cycle.
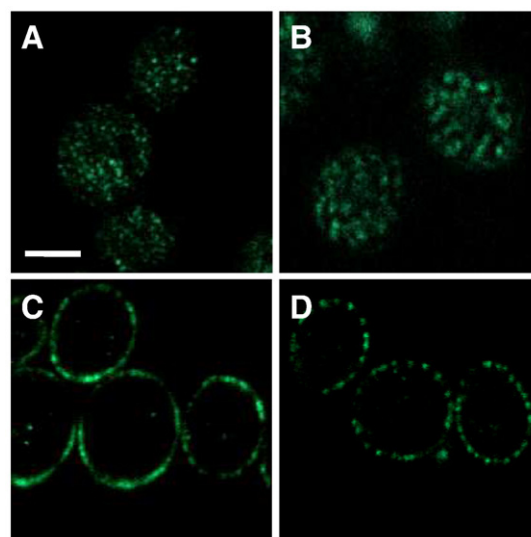

Fig. 7. Evolution of the repartition of Sur7-GFP after rehydration. (A) and (B) correspond to cells after shock to 166 MPa, kept during 60 min in hyperosmotic conditions followed by shock rehydration to 1.4 MPa. (C) and (D) correspond to cells after slope dehydration to 166 MPa, kept 60 min in hyperosmotic conditions followed by progressive rehydration to 1.4 MPa. Cells were observed just after rehydration (A and C) or 90 min after rehydration (B and D). Bar scale = 2 μm.

Table 3
Impact of different dehydration kinetics to 166 MPa on the number and size of plasma membrane domain containing Sur7-GFP.

	Mean number (SD) of domains by cell section	Mean size of domain (μm)
Control 1.4 MPa	11.0 (0.6)	0.56 (0.05)
Shock 166 MPa	11.0 (1.6)	0.49 (0.015)
Slope 166 MPa	6.3 (0.8)	1.13 (0.24)

The mean number of domains was estimated by observation of median optical sections through the cells. The SDs were calculated from the observation of 20 cells for each treatment.
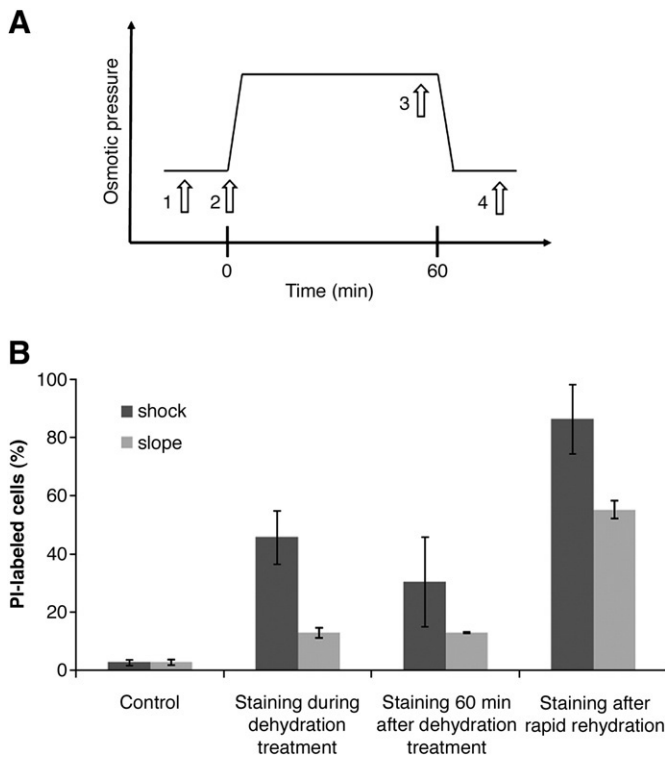
Fig. 8. Estimation of the integrity of yeast during dehydration–rehydration. (A) Protocol for cell staining with PI in order to investigate the evolution of membrane permeability during treatments. The arrows represent the timing of cell staining: 0 min corresponds to the beginning of the hyperosmotic treatment. PI was introduced (1) before, (2) during, (3) 60 min after the dehydration treatment, and (4) after the rehydration step. Rapid dehydration (shock) and progressive dehydration (slope) were performed. (B) The proportion of permeabilized cells (positively stained with PI) during and 60 min after 166 MPa dehydration treatment, and after rapid rehydration to 1.4 MPa. Error bars correspond to the SD calculated from three repeat experiments. At least 300 cells were observed for each experiment.

The cause of membrane internalization after severe hyperosmotic shock may be related to the rapid volume contraction of the cells. Due to the low lateral compressibility of the membrane [46], the cell s/v ratio increase conducted to the deformation of the plasma membrane [9,10]. After severe hyperosmotic shocks, the dissipation of membrane surface excess could be achieved by undulation and furrow-like invaginations of the plasma membrane. Furrow-like invaginations, localized at the MCC domains containing Sur7p [36], were also observed in our study in isotonic conditions (Fig. 5B) but they were shallower than after hyperosmotic shocks (Fig. 5D). A possible mechanism is the extension of membrane invaginations, existing in isotonic conditions, to dissipate the excess of membrane surface. This assumption is supported by the observation of the closeness of the Sur7-GFP patches after the shock dehydration (Table 3). Observation of Sur7-GFP localized in sterol-rich MCC microdomains revealed that these proteins were not internalized (Fig. 6B). Consequently, the phenomenon of membrane internalization could consist in a first initial step of furrow-like invagination extension by low sterol content membrane region. Membrane fusion is the second step necessary for membrane internalization. This event could be explained by the closeness between two portions of plasma membrane (Fig. 5D), protein aggregation [47] and the structural instability of lipids in hyperosmotic conditions which promote membrane fusion and vesicle formation [48,49].

4.3. Progressive dehydrations and cell survival to severe treatments (110 and 166 MPa)

As already reported [13,22,23], progressive dehydrations allow higher survival rates than ones obtained after rapid treatments

(Table 2). High cell survival rates are related to the preservation of plasma membrane integrity during the two steps of dehydration–rehydration cycle (Fig. 8). Preservation of membrane continuity may result from the particular evolution of membrane structure during progressive perturbations which consists in the formation of big pleats. Accordingly, membrane surface excess, caused by cell volume contraction, is dissipated in some fewer and larger pleats than in the case of shock dehydration (Fig. 5). Such deformations do not bring closer portions of plasma membrane which could explain the absence of membrane internalization over time after progressive treatments (Fig. 4).

The formation of these large invaginations which curled back toward the cell surface (Fig. 5E and F) could be related to the rate of increase of the s/v ratio. Indeed, such invaginations are sometimes observed when the chemical fixation of samples for electron microscopy causes slight osmotic dehydration. Similar formations are also observed on yeast mutants presenting an imbalance between exocytosis and endocytosis which is not compensated by a parallel increase in overall growth [50]. In this last case, the increase of the s/v ratio also occurs progressively. Formation of such invaginations could depend on the time required for the lateral reorganization of the plasma membrane. This hypothesis is comforted by the observation of the modification of Sur7-GFP repartition after the progressive dehydration (Fig. 6). Delocalization of proteins located in MCC domains after perturbation has been already reported: plasma membrane depolarization induces reversible dispersion of the H$^+$-symporters, localized in MCC domains in physiological conditions [19]. However, to our knowledge, the delocalization of Sur7p has never been observed. Sur7p is described as a very stable protein due to its association with large immobile protein assemblies at the cell cortex [51]. Observation of its redistribution could be linked to the severity of the perturbation used in the present study. Indeed, modification of Sur7p lateral distribution, after progressive dehydration to 166 MPa, could be related to thorough membrane reorganization caused by the disordered to ordered phase transition which occurs in this elevated range of osmotic pressures [12]. Such phenomenon is known to promote progressive phase separation in the membrane plane [52] and could influence the lateral distribution of proteins in the membrane due to their partition equilibrium between phases [53].

After progressive dehydration, invaginations formed during the perturbation could be reincorporated into the plasma membrane during rehydration, avoiding permeabilization for some of the cells during the increase in cell volume (Table 2). The survival rate of yeasts was even higher when rehydration was performed progressively, as already reported on bacteria [54]. Hypothetical events that may allow a high survival rate during severe dehydration followed by rehydration are presented in Fig. 9B. Progressive rehydration probably causes slow and optimal unfolding of membrane pleats which allows the maintenance of membrane integrity. This explains the beneficial effect on yeast survival of rehydration in the slope condition after dehydration to 166 MPa (Table 2). Therefore, after dehydration to high-osmotic pressures, the rehydration step should be considered as a second perturbation. After rehydration, the MCC domains visualized by Sur7-GFP did not immediately appear as small domains but recovered their patch distribution over time (Fig. 7). The time period after rehydration, allowing Sur7-GFP patch recovery, could correspond to the requisite time for the recovery of the cell metabolism after hydric perturbations which could be involved in rich Sur7p domain re-formation. However, this mechanism is not really understood and should be investigated further.

5. Conclusion

The present study focused on yeast plasma membrane modifications and their dynamics during hyperosmotic perturbations. We found that the modifications varied according to the osmotic level and
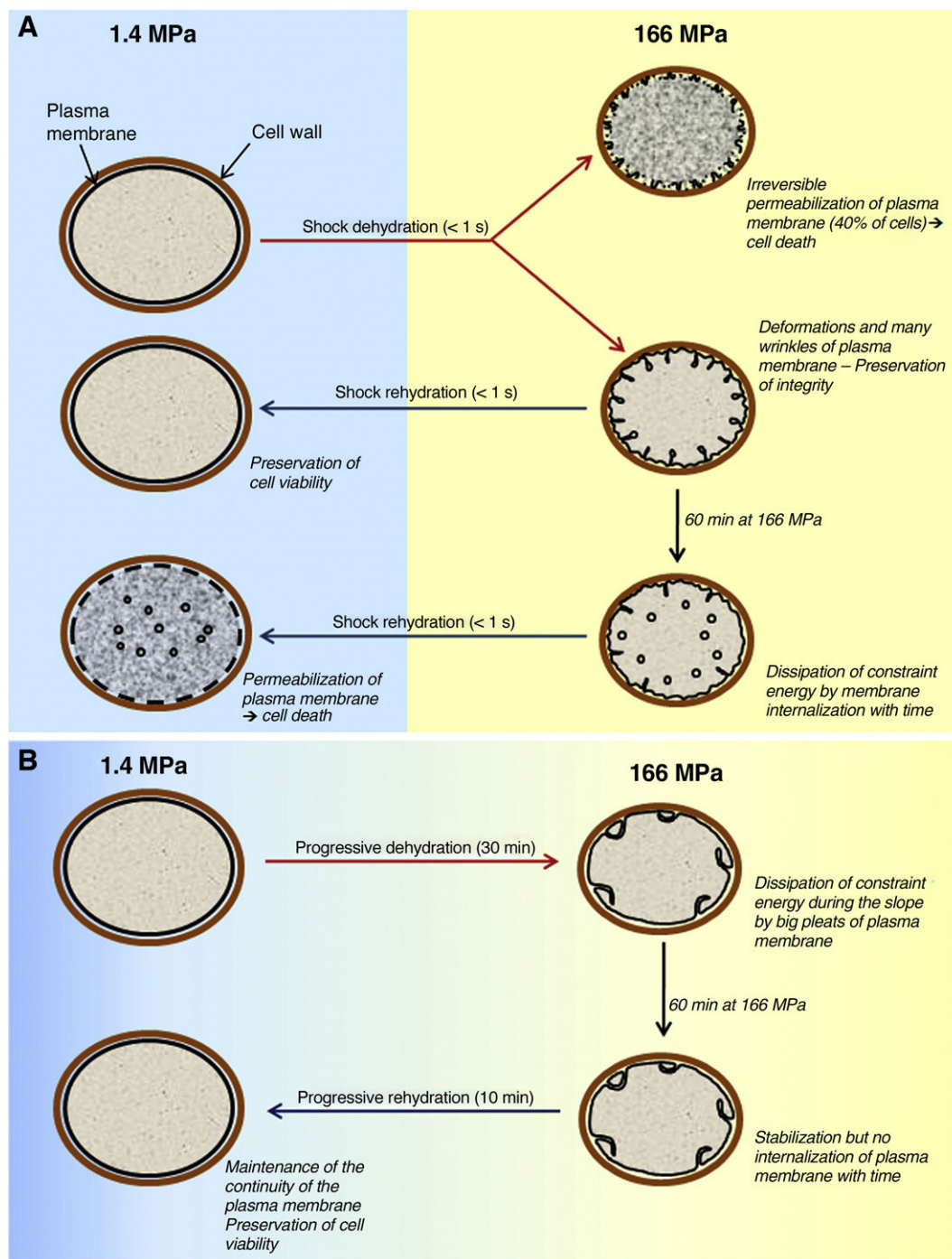
Fig. 9. Schematic representations of the hypothetical sequence of events occurring during high-amplitude dehydration of yeast in the shock (A) or slope (B) conditions followed by rehydration. The first scheme (A) highlights the different mechanisms leading to cell death during the rapid dehydration and rehydration stages. Scheme B explains how the yeasts maintain their integrity during progressive dehydration followed by progressive rehydration.

the kinetic of treatment and could explain the survival and the death of cells during hydric perturbations. The study of plasma membrane behavior during drastic hydric perturbations showed that cell death is strongly related to loss of membrane integrity. A determinant mechanism causing the loss of membrane integrity during dehydration–rehydration cycle is a plasma membrane internalization which occurs after hyperosmotic shocks. We have shown for the first time that the morphologic response of the plasma membrane is related to the kinetic of dehydration, suggesting that this cellular structure is sensitive to the rate of environmental perturbation. By visualizing the dynamics of the membrane microdomains during environmental

perturbation, we have shown that lateral membrane reorganization can occur during hydric disturbance and that this organization is time dependent. This suggests that the plasticity of the plasma membrane is a key property in the resistance of cells to environmental stresses. Such knowledge may lead to improvement of cell resistance during hydric stress and to optimization of preservation methods based on dehydration (drying, freezing, and freeze-drying). Indeed, the both steps of the dehydration–rehydration cycle need to be considered as critical for membrane integrity and cell survival. Future studies will focus on the mechanisms of plasma membrane lateral reorganization during drastic environmental perturbation and the potential effects of

lipid structural transitions and changes in functionality of active proteins on the membrane microdomain distribution.

Acknowledgements

References

[1] K.L. Scott, J. Lecak, J.P. Acker, Biopreservation of red blood cells: past, present, and future, Transfus. Med. Rev. 19 (2005) 127–142.

[2] X.C. Meng, C. Stanton, G.F. Fitzgerald, C. Daly, R.P. Ross, Anhydrobiotics: the challenges of drying probiotic cultures, Food Chem. 106 (2008) 1406–1416.

[3] C.A. Morgan, N. Herman, P.A. White, G. Vesey, Preservation of micro-organisms by drying; a review, J. Microbiol. Methods 66 (2006) 183–193.

[4] E. Klipp, B. Nordlander, R. Kruger, P. Gennemark, S. Hohmann, Integrative model of the response of yeast to osmotic shock, Nat. Biotechnol. 23 (2005) 975–982.

[5] P.A. Marechal, I.M. de Maranon, P. Molin, P. Gervais, Yeast cell responses to water potential variations, Int. J. Food Microbiol. 28 (1995) 277–287.

[6] S.J. Prestrelski, N. Tedeschi, T. Arakawa, J.F. Carpenter, Dehydration-induced conformational transitions in proteins and their inhibition by stabilizers, Biophys. J. 65 (1993) 661–671.

[7] B. van den Berg, R.J. Ellis, C.M. Dobson, Effects of macromolecular crowding on protein folding and aggregation, EMBO J. 18 (1999) 6927–6933.

[8] P. Gervais, L. Beney, Osmotic mass transfer in the yeast *Saccharomyces cerevisiae*, Cell. Mol. Biol. 47 (2001) 831–839.

[9] A.K. Adya, E. Canetta, G.M. Walker, Atomic force microscopic study of the influence of physical stresses on *Saccharomyces cerevisiae* and *Schizosaccharomyces pombe*, FEMS Yeast Res. 6 (2006) 120–128.

[10] F. Guilak, G.R. Erickson, H.P. Ting-Beall, The effects of osmotic stress on the viscoelastic and physical properties of articular chondrocytes, Biophys. J. 82 (2002) 720–727.

[11] J.H. Crowe, F.A. Hoekstra, L.M. Crowe, Membrane phase transitions are responsible for imbibitional damage in dry pollen, Proc. Natl. Acad. Sci. USA 86 (1989) 520–523.

[12] C. Laroche, L. Beney, P.A. Marechal, P. Gervais, The effect of osmotic pressure on the membrane fluidity of *Saccharomyces cerevisiae* at different physiological temperatures, Appl. Microbiol. Biotechnol. 56 (2001) 249–254.

[13] V. Ragoonanan, J. Malsam, D.R. Bond, A. Aksan, Roles of membrane structure and phase transition on the hyperosmotic stress survival of *Geobacter sulfurreducens*, Biochim. Biophys. Acta 1778 (2008) 2283–2290.

[14] M.J. Beker, A.I. Rapoport, Conservation of yeasts by dehydration, Adv. Biochem. Eng. Biotechnol. 35 (1987) 127–171.

[15] A.I. Rapoport, G.M. Khroustalyova, E.N. Kuklina, Anhydrobiosis in yeast: activation effect, Braz. J. Med. Biol. Res. 30 (1997) 9–13.

[16] H. Simonin, L. Beney, P. Gervais, Sequence of occurring damages in yeast plasma membrane during dehydration and rehydration: mechanisms of cell death, Biochim. Biophys. Acta 1768 (2007) 1600–1610.

[17] K. Simons, E. Ikonen, Functional rafts in cell membranes, Nature 387 (1997) 569–572.

[18] F.R. Maxfield, Plasma membrane microdomains, Curr. Opin. Cell Biol. 14 (2002) 483–487.

[19] G. Grossmann, M. Opekarova, J. Malinsky, I. Weig-Meckl, W. Tanner, Membrane potential governs lateral segregation of plasma membrane proteins and lipids in yeast, EMBO J. 26 (2007) 1–8.

[20] K. Malinska, J. Malinsky, M. Opekarova, W. Tanner, Visualization of protein compartmention within the plasma membrane of living yeast cells, Mol. Biol. Cell 14 (2003) 4427–4436.

[21] G. Grossmann, J. Malinsky, W. Stahlschmidt, M. Loibl, I. Weig-Meckl, W.B. Frommer, M. Opekarova, W. Tanner, Plasma membrane microdomains regulate turnover of transport proteins in yeast, J. Cell Biol. 183 (2008) 1075–1088.

[22] P. Mary, D. Ochin, R. Tailliez, Rates of drying and survival of *Rhizobium meliloti* strains during storage at different relative humidities, Appl. Environ. Microbiol. 50 (1985) 207–211.

[23] L. Beney, I. Martinez de Maranon, P.A. Marechal, P. Gervais, Influence of thermal and osmotic stresses on the viability of the yeast *Saccharomyces cerevisiae*, Int. J. Food Microbiol. 55 (2000) 275–279.

[24] Y. Mille, J.P. Obert, L. Beney, P. Gervais, New drying process for lactic bacteria based on their dehydration behavior in liquid medium, Biotechnol. Bioeng. 88 (2004) 71–76.

[25] C. Schlee, M. Miedl, K.A. Leiper, G.G. Stewart, The potential of confocal imaging for measuring physiological changes in Brewer's yeast, J. Inst. Brew. 112 (2006) 134–147.

[26] J.C. Anand, A.D. Brown, Growth rate patterns of the so-called osmophilic and non-osmophilic yeasts in solutions of polyethylene glycol, J. Gen. Microbiol. 52 (1968) 205–212.

[27] H. Ito, Y. Fukada, K. Murata, A. Kimura, Transformation of intact yeast cells treated with alkali cations, J. Bacteriol. (1983) 163–168.

[28] R.S. Norrish, An equation for the activity coefficients and equilibrium relative humidities of water in confectionery syrups, Int. J. Food Sci. Technol. 1 (1966) 25–39.

[29] J. Chirife, C.F. Fontan, A study of the water activity lowering behavior of polyethylene glycols in the intermediate moisture range, J. Food Sci. 45 (1980) 1717–1719.

[30] Y. Gachet, J.S. Hyams, Endocytosis in fission yeast is spatially associated with the actin cytoskeleton during polarised cell growth and cytokinesis, J. Cell Sci. 118 (2005) 4231–4242.

[31] T. Meckel, A.C. Hurst, G. Thiel, U. Homann, Endocytosis against high turgor: intact guard cells of *Vicia faba* constitutively endocytose fluorescently labelled plasma membrane and GFP-tagged K-channel KAT1, Plant J. 39 (2004) 182–193.

[32] T.A. Vida, S.D. Emr, A new vital stain for visualizing vacuolar membrane dynamics and endocytosis in yeast, J. Cell Biol. 128 (1995) 779–792.

[33] J.P. Thiery, Mise en evidence des polysaccharides sur coupes fines en microscopie electronique, J. Microsc. 6 (1967) 987–1018.

[34] D. Otsuga, B.R. Keegan, E. Brisch, J.W. Thatcher, G.J. Hermann, W. Bleazard, J.M. Shaw, The dynamin-related GTPase, Dnm1p, controls mitochondrial morphology in yeast, J. Cell Biol. 143 (1998) 333–349.

[35] H. Riezman, Endocytosis in yeast: several of the yeast secretory mutants are defective in endocytosis, Cell 40 (1985) 1001–1009.

[36] V. Stradalova, W. Stahlschmidt, G. Grossmann, M. Blazikova, R. Rachel, W. Tanner, J. Malinsky, Furrow-like invaginations of the yeast plasma membrane correspond to membrane compartment of Can1, J. Cell Sci. 122 (2009) 2887–2894.

[37] Q. Bone, E.J. Denton, The osmotic effects of electron microscope fixatives, J. Cell Biol. 49 (1971) 571–581.

[38] M. Ferrando, W.E.L. Spiess, Cellular response of plant tissue during the osmotic treatment with sucrose, maltose, and trehalose solutions, J. Food Eng. 49 (2001) 115–127.

[39] G.J. Morris, L. Winters, G.E. Coulson, K.J. Clarke, Effect of osmotic stress on the ultrastructure and viability of the yeast *Saccharomyces cerevisiae*, J. Gen. Microbiol. 132 (1986) 2023–2034.

[40] M.E. Young, T.S. Karpova, B. Brugger, D.M. Moschenross, G.K. Wang, R. Schneiter, F.T. Wieland, J.A. Cooper, The Sur7p family defines novel cortical domains in *Saccharomyces cerevisiae*, affects sphingolipid metabolism, and is involved in sporulation, Mol. Cell. Biol. 22 (2002) 927–934.

[41] A.M. Robertson, I.M. Hagan, Stress-regulated kinase pathways in the recovery of tip growth and microtubule dynamics following osmotic stress in *S. pombe*, J. Cell Sci. 121 (2008) 4055–4068.

[42] I. Slaninova, S. Sestak, A. Svoboda, V. Farkas, Cell wall and cytoskeleton reorganization as the response to hyperosmotic shock in *Saccharomyces cerevisiae*, Arch. Microbiol. 173 (2000) 245–252.

[43] K.R. Ayscough, J. Stryker, N. Pokala, M. Sanders, P. Crews, D.G. Drubin, High rates of actin filament turnover in budding yeast and roles for actin in establishment and maintenance of cell polarity revealed using the actin inhibitor latrunculin-A, J. Cell Biol. 137 (1997) 399–416.

[44] D. Pruyne, A. Bretscher, Polarization of cell growth in yeast, J. Cell Sci. 113 (Pt 4) (2000) 571–585.

[45] S. Garcia-Manyes, G. Oncins, F. Sanz, Effect of temperature on the nanomechanics of lipid bilayers studied by force spectroscopy, Biophys. J. 89 (2005) 4261–4274.

[46] E.A. Evans, R. Waugh, L. Melnik, Elastic area compressibility modulus of red cell membrane, Biophys. J. 16 (1976) 585–595.

[47] K. Goyal, L.J. Walton, A. Tunnacliffe, LEA proteins prevent protein aggregation due to water stress, Biochem. J. 388 (2005) 151–157.

[48] J. Liu, M. Kaksonen, D.G. Drubin, G. Oster, Endocytic vesicle scission by lipid phase boundary forces, Proc. Natl. Acad. Sci. USA 103 (2006) 10277–10282.

[49] A. Roux, D. Cuvelier, P. Nassoy, J. Prost, P. Bassereau, B. Goud, Role of curvature and phase transition in lipid sorting and fission of membrane tubules, EMBO J. 24 (2005) 1537–1545.

[50] B. Singer-Kruger, Y. Nemoto, L. Daniell, S. Ferro-Novick, P. De Camilli, Synaptojanin family members are implicated in endocytic membrane traffic in yeast, J. Cell Sci. 111 (1998) 3347–3356.

[51] T.C. Walther, J.H. Brickner, P.S. Aguilar, S. Bernales, C. Pantoja, P. Walter, Eisosomes mark static sites of endocytosis, Nature 439 (2006) 998–1003.

[52] K. Jorgensen, O.G. Mouritsen, Phase-separation dynamics and lateral organization of 2-component lipid-membranes, Biophys. J. 69 (1995) 942–954.

[53] T. Baumgart, A.T. Hammond, P. Sengupta, S.T. Hess, D.A. Holowka, B.A. Baird, W.W. Webb, Large-scale fluid/fluid phase separation of proteins and lipids in giant plasma membrane vesicles, Proc. Natl. Acad. Sci. USA 104 (2007) 3165–3170.

[54] Y. Mille, L. Beney, P. Gervais, Magnitude and kinetics of rehydration influence the viability of dehydrated *E. coli* K-12, Biotechnol. Bioeng. 83 (2003) 578–582.